

Clathrin recruits phosphorylated TACC3 to spindle poles for bipolar spindle assembly and chromosome alignment

Wenxiang Fu^{1,*}, Wei Tao^{1,*}, Puwei Zheng¹, Jingyan Fu¹, Minglei Bian¹, Qing Jiang¹, Paul R. Clarke² and Chuanmao Zhang^{1,‡}

¹The MOE Key Laboratory of Cell Proliferation and Differentiation and the State Key Laboratory of Bio-membrane and Membrane Bioengineering, College of Life Sciences, Peking University, Beijing 100871, China

²Biomedical Research Institute, College of Medicine, Dentistry and Nursing, Ninewells Hospital and Medical School, University of Dundee, Dundee DD1 9SY, UK

*These authors contributed equally to this work

‡Author for correspondence (zhangcm@pku.edu.cn)

Accepted 5 July 2010

Journal of Cell Science 123, 3645–3651

© 2010. Published by The Company of Biologists Ltd

doi:10.1242/jcs.075911

Summary

Transforming acidic coiled-coil-containing protein 3 (TACC3) has been implicated in mitotic spindle assembly, although the mechanisms involved are largely unknown. Here we identify that clathrin heavy chain (CHC) binds specifically to phosphorylated TACC3 and recruits it to spindle poles for proper spindle assembly and chromosome alignment. Phosphorylation of *Xenopus* TACC3 at serine 620 (S620) and S626, but not S33, is required for its binding with CHC. Knockdown of CHC by RNA interference (RNAi) abolishes the targeting of TACC3 to spindle poles and results in abnormal spindle assembly and chromosome misalignment, similar to the defects caused by TACC3 knockdown. Furthermore, the binding of CHC with phosphorylated TACC3 is inhibited by importin β and this inhibition is reversed by the presence of the GTP-binding nuclear protein Ran in the GTP-bound state. Together, these results indicate that the recruitment of phosphorylated TACC3 to spindle poles by CHC ensures proper spindle assembly and chromosome alignment, and is regulated by Ran.

Key words: TACC3, Clathrin, Phosphorylation, Spindle assembly, Chromosome alignment

Introduction

The transforming acidic coiled-coil-containing (TACC) family proteins share a highly conserved TACC motif close to their C terminus and have been linked to mitosis (Jung et al., 2006; Lauffart et al., 2005; Raff, 2002). Members of this family include TACC in *Drosophila*, TACC3 (maskin) in *Xenopus*, and TACC1, TACC2 and TACC3 in humans (Gergely et al., 2000a; Gergely et al., 2000b; Stebbins-Boaz et al., 1999). It is generally accepted that the function of TACC3 in spindle assembly depends on its enrichment (by phosphorylation) at mitotic spindle poles. For example, *Xenopus* TACC3 (xTACC3) phosphorylated by Aurora kinase A (Aurora A) at serine residues 33 (S33), S620 and S626 regulates microtubule polymerization at centrosomes and functions in centrosome-dependent mitotic spindle assembly in *Xenopus* egg extract (Kinoshita et al., 2005; O'Brien et al., 2005; Peset et al., 2005). As in *Xenopus* cells, human TACC3 (hTACC3) is also phosphorylated by Aurora A at a site that is equivalent to S626 in xTACC3 (S558), and the phosphorylated hTACC3 targets to spindle poles in response to functional requirement (LeRoy et al., 2007). However, the molecular basis of the targeting of TACC3 to spindle poles during mitosis and its role in spindle function have not been established.

Clathrin has a crucial role in the trafficking of endocytic vesicles (Kaksonen et al., 2005; Pucadyil and Schmid, 2009; Takei and Haucke, 2001). Three clathrin heavy chains (CHCs) and three clathrin light chains (CLCs) form triskelia, which assemble into a lattice-like coat around membrane vesicles and have an important function during endocytosis in interphase cells (Fotin et al., 2004a; Fotin et al., 2004b). Interestingly, clathrin has also been reported

to be required for spindle assembly and kinetochore fiber stabilization in mitotic cells (Royle et al., 2005; Royle and Lagnado, 2006; Tahara et al., 2007; Yamauchi et al., 2008), but the mechanism of action remains largely unknown.

We found that TACC3 phosphorylated by Aurora A specifically binds to CHC in both human and *Xenopus* cells. Binding is inhibited by importin β , and GTP-bound Ran (RanGTP) can reverse the inhibition. Importantly, the recruitment of phosphorylated TACC3 to the spindle poles by CHC requires the interaction between TACC3 and CHC. The depletion of CHC by RNA interference (RNAi) leads not only to mislocalization of endogenous TACC3 at spindle poles, but also to defects in both bipolar spindle assembly and chromosome alignment. Thus, our data reveal that the recruitment of phosphorylated TACC3 to spindle poles by clathrin ensures proper bipolar spindle assembly and chromosome alignment in mitotic cells through a RanGTP-dependent pathway.

Results and Discussion

Phosphorylated TACC3 specifically interacts with CHC in a RanGTP-regulated manner

To identify binding partners of phosphorylated TACC3, we first analyzed precipitated proteins by glutathione *S*-transferase (GST) pull-down using GST-bound full-length xTACC3 (GST-xTACC3) and xTACC3-dNT1 [amino acids (aa) 366–931] (GST-xTACC3-dNT1) in *Xenopus* cytosolic factor (CSF) extract in the presence or absence of Aurora A (Fig. 1A,B). Using SDS-PAGE, we observed that an ~180 kDa polypeptide specifically interacted with xTACC3-dNT1 wild type (WT) in the presence of Aurora A, and

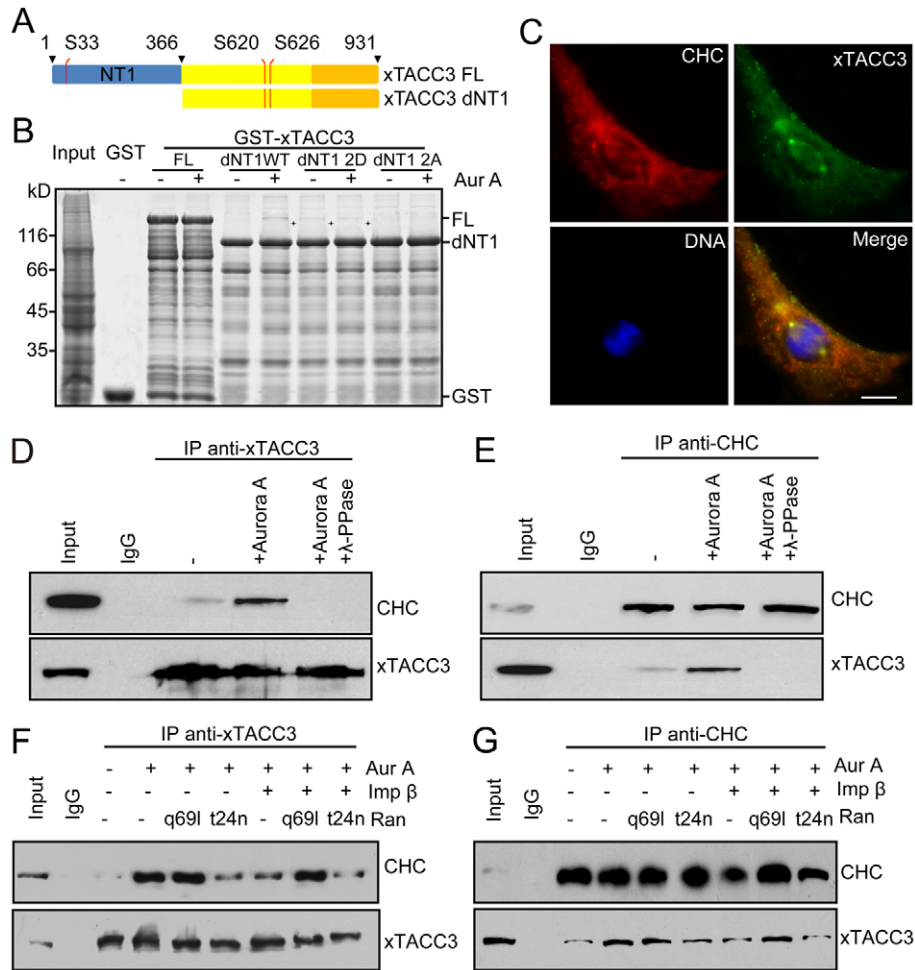


Fig. 1. Phosphorylated xTACC3 specifically interacts with CHC in a RanGTP-regulated manner. (A) Schematic of the xTACC3 constructs used: xTACC3-FL (aa 1–931) and xTACC3-dNT1 (aa 366–931). Three serines (S33, S620 and S626) that are phosphorylated by Aurora A are marked with red lines. Blue, N-terminal domain fragment 1; yellow, N-terminal domain fragment 2; orange, C-terminal TACC domain. (B) CHC was identified as a binding protein of phosphorylated xTACC3-dNT1. A co-precipitation assay was performed with GST-xTACC3 full-length wild type (FL), xTACC3-dNT1 wild-type (dNT1 WT) and phospho-mimetic mutants (dNT1 2D and dNT1 2A) with or without Aurora A kinase (1 μ M) in CSF extracts. Elsewhere within the blots, + marks a 180-kDa peptide band, which was identified as CHC by using MALDI-TOF mass spectrometry. (C) CHC colocalizes with xTACC3 at spindle microtubules and spindle poles in methanol-fixed XTC cells. CHC is shown in red, xTACC3 in green and DNA in blue. Scale bar: 10 μ m. (D,E) Co-immunoprecipitation assays were performed in CSF extracts using anti-xTACC3 (D) or anti-CHC (E) antibodies in the presence or absence of Aurora A and λ -PPase. Input and immunoprecipitates were probed with anti-CHC (upper) and anti-xTACC3 (lower) antibodies. (F,G) Co-immunoprecipitation assays were performed using anti-xTACC3 (F) and anti-CHC (G) antibodies in CSF extracts with a combination of exogenous purified Aurora A (1 μ M), RanQ69L (2 μ M), RanT24N (2 μ M) and importin β (1 μ M) as indicated. The blots were probed with anti-CHC (upper) and anti-xTACC3 (lower) antibodies.

this polypeptide was masked by GST-xTACC3 (Fig. 1B). Through point mutation analysis, we found that the phosphorylation mimetic mutants S620D and S626D of xTACC3 (xTACC3-dNT1 2D), but not the non-phosphorylatable double mutant S620A and S626A (S620A/S626A, dNT1 2A), bound with the polypeptide in both the presence or absence of Aurora A, suggesting that binding depends on the phosphorylation state of xTACC3 (Fig. 1B). Analysis by matrix-assisted laser desorption/ionization time-of-flight (MALDI-TOF) mass spectrometry identified this polypeptide as CHC. Immunofluorescence labeling showed that xTACC3 and CHC colocalized on the mitotic spindle in *Xenopus* tissue culture (XTC) cells and were concentrated together on the spindle poles (Fig. 1C). We also observed that CHC bound very weakly to xTACC3 in *Xenopus* CSF extracts and this interaction was greatly enhanced by the addition of Aurora A (Fig. 1D). When λ -protein phosphatase (λ -PPase) was added to the extract, the interaction was completely abolished, indicating that the interaction requires phosphorylation of xTACC3 by Aurora A (Fig. 1D). We performed a reciprocal experiment and observed that xTACC3 immunoprecipitated with CHC and that Aurora A also greatly enhanced the interaction (Fig. 1E). Furthermore, sucrose gradient fractionation of CSF extracts confirmed that xTACC3 and CHC were present in the same fractions under native low-salt conditions, and that the interaction was enhanced by Aurora A, i.e. a larger protein complex was formed (supplementary material Fig. S1).

It has been reported that phosphorylation of xTACC3 by Aurora A is regulated by Ran GTPase and importin β (Albee et al., 2006). To test whether the interaction between CHC and phosphorylated xTACC3 is also regulated by Ran GTPase and importin β , we immunoprecipitated xTACC3 from CSF extracts in the presence of RanQ69L (stabilized in the GTP-bound state), RanT24N (which fails to bind GTP, forms an inhibitory complex with the regulator of chromosome condensation RCC1 and has a dominant inhibitory effect on the generation of Ran-GTP) (Dasso et al., 1994; Klebe et al., 1995) and/or importin β (Fig. 1F). We found that importin β inhibited the interaction between xTACC3 and CHC. This inhibition was reversed by RanQ69L but not by RanT24N (Fig. 1F). A reciprocal experiment also showed that importin β inhibited the interaction and that the inhibition could be reversed by RanGTP (Fig. 1G). Together, these data demonstrate that CHC interacts specifically with phosphorylated xTACC3 in *Xenopus* CSF extracts in a RanGTP-regulated manner.

Phosphorylation of xTACC3 at S620 and S626, but not S33, is required for binding with CHC and functions in RanGTP-dependent spindle assembly

It has been shown that three sites (S33, S620 and S626) of xTACC3 are phosphorylated by Aurora A (Peset et al., 2005); we confirmed this (supplementary material Fig. S2A) and then tested the role of each of the three sites in the interaction with CHC. Through point

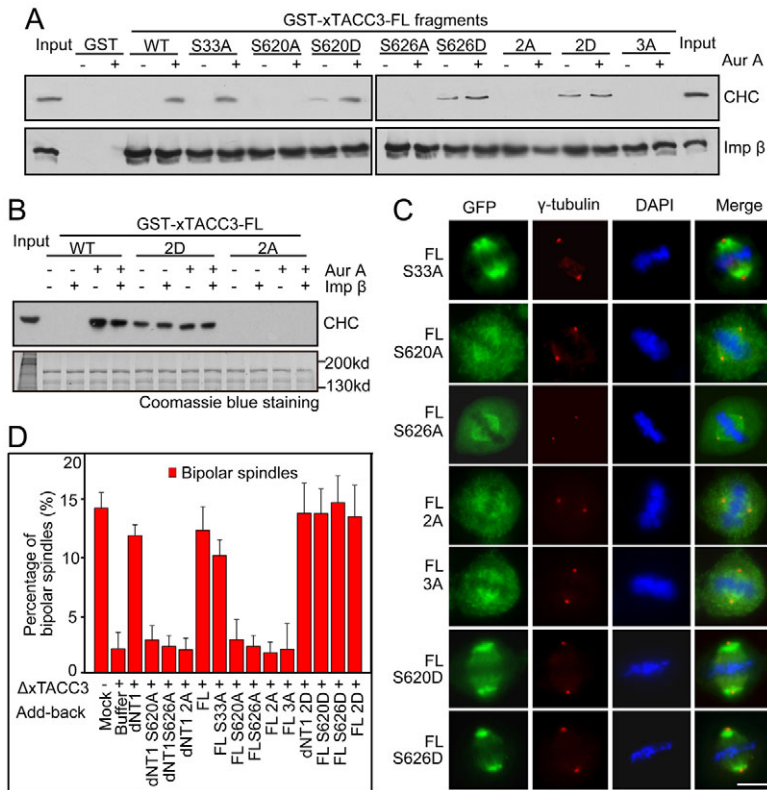


Fig. 2. Phosphorylation of xTACC3 at S620 and S626, but not at S33, is required for binding with CHC and function in RanGTP-dependent spindle assembly. (A) Co-precipitation assays using GST-xTACC3 full-length (FL) wild type (WT) and phospho-mimetic mutants in the presence or absence of Aurora A, as indicated. The blots were probed with anti-CHC (upper) and anti-importin- β (lower). (B) GST-xTACC3 FL WT, FL 2D and FL 2A bound to Sepharose beads were incubated in the CSF extract with combinations of Aurora A (1 μ M) and importin β (1 μ M) as indicated. The precipitates were probed with anti-CHC antibody (upper) and stained with Coomassie Blue (lower) to show the major band corresponding to the GST-FL proteins. (C) GFP-tagged xTACC3-FL WT and mutants were transiently transfected into HeLa cells and representative micrographs are shown. GST-xTACC3-FL WT, S33A, S620D and S626D mainly localized to spindles, with strong immunofluorescence staining at poles, whereas other constructs showed weak localization to spindle microtubules and no accumulation at spindle poles. xTACC3 is shown in green, γ -tubulin in red and DNA in blue. Scale bar: 10 μ m. (D) RanGTP-induced bipolar spindles assembled in mock-depleted and xTACC3-depleted extracts with add-back of xTACC3 phosphorylation mutants, including dNT1 WT, dNT1 S620A, dNT1 S626A, dNT1 2A, FL WT, FL S33A, FL S620A, FL S626A, FL 2A, FL 3A, dNT1 2D, FL S620D, FL S626D and FL 2D. Quantification of the percentage of RanGTP-induced bipolar spindles assembled is shown. RanGTP-mediated bipolar spindle assembly is ensured by phosphorylation at S620 and S626, but phosphorylation of S33 is not required. Data are means \pm s.d.

mutation, we found that the S620A mutant bound CHC only weakly even in the presence of Aurora A, whereas the S626A mutant and double mutant FL 2A did not bind at all (Fig. 2A). The single phospho-mimetic mutant S620D or S626D interacted with CHC even in the absence of Aurora A, and their interaction was enhanced by excess Aurora A. When S620 and S626 were phospho-mimetically double mutated to aspartic acid, the interaction with CHC was not enhanced further by Aurora A. By contrast, the S33A mutation had no effect on the interaction (Fig. 2A). These findings indicate that phosphorylation of S620 and S626 by Aurora A is required for the interaction between xTACC3 and CHC, but S33 phosphorylation is not required. These results were also confirmed using xTACC3-dNT1 (Fig. S2B); results indicate that the NT1 domain and its phosphorylation state at S33 are not required for the interaction between xTACC3 and CHC. Furthermore, the binding of the double phospho-mimetic mutant FL 2D to CHC was not affected by the addition of Aurora A and/or importin β . The non-phosphorylatable double mutant FL 2A did not bind to CHC at all (Fig. 2B). xTACC3-dNT1 showed consistently similar characteristics to full-length xTACC3 in binding to CHC and for this binding being regulated by Aurora A and importin β (supplementary material Fig. S2C).

Consistent with the result that S33 phosphorylation is unnecessary for the binding of xTACC3 to CHC, we found that phosphorylation of S620 and S626, but not S33, is required for the targeting of xTACC3 to spindle poles in vivo (Fig. 2C). We constructed green fluorescent protein (GFP)-xTACC3 fusion proteins in which each of the three sites (S620, S626 and S33) was mutated to either non-phosphorylatable (alanine) or phospho-mimetic (aspartate) residues. When expressed in HeLa cells, the mutant xTACC3 S33A localized normally to the mitotic spindle with a concentration at the poles similar to that of wild-type

xTACC3. By contrast, the mutants S620A, S626A, S620A/S626A (FL 2A) and S33A/S620A/S626A (FL 3A) all failed to concentrate at spindle poles, and instead localized to the spindle microtubules and partially dispersed in the cytoplasm. The phospho-mimetic mutants S620D and S626D both concentrated at the spindle poles, as did wild-type xTACC3 and xTACC3 S33A (Fig. 2C). Similarly, xTACC3-dNT1, which lacks the S33 site, showed normal enrichment at spindle poles (supplementary material Fig. S2D). These observations strongly suggest that phosphorylation of S620 and S626, but not of S33, is required for the targeting of xTACC3 to spindle poles in vivo. To rule out the possibility that the targeting failure of non-phosphorylatable mutants to spindle poles is due to the loss of ability to bind centrosomal proteins or microtubules, we tested the interactions between the purified non-phosphorylatable mutants and the centrosomal protein γ -tubulin, and the interactions between the nonphosphorylatable mutants and microtubules. We found that all of the non-phosphorylatable mutants of xTACC3 could bind to γ -tubulin in *Xenopus* CSF extracts, and taxol stabilized microtubules in vitro (supplementary material Fig. S3A–C).

The fact that S33 is not required for the targeting of xTACC3 to spindle poles suggests that phosphorylation of S33 is irrelevant to spindle formation. *Xenopus* egg CSF extract supports bipolar spindle assembly in vitro without chromatin in the presence of RanGTP (RanQ69L) (Carazo-Salas et al., 1999; Wilde and Zheng, 1999). We found that the ability to form bipolar spindles in the presence of RanQ69L was abolished in xTACC3-depleted extracts, and this ability was fully restored by full-length wild-type xTACC3, by the phospho-mimetic mutant and by the non-phosphorylatable mutant S33A but not by the non-phosphorylatable mutants dNT1 2A (supplementary material Fig. S2E,F; Fig. 2D). These results indicate that the role of xTACC3 in bipolar spindle formation requires the phosphorylation of S620 and S626 but not S33.

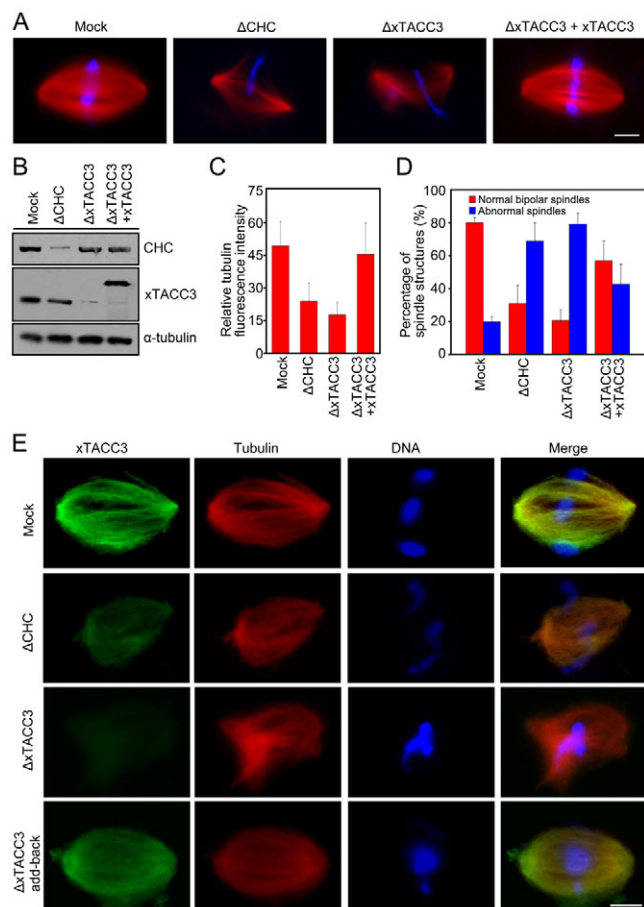


Fig. 3. CHC recruits xTACC3 to spindle poles for proper bipolar spindle assembly. (A) Sperm-induced spindles were assembled in mock-depleted, CHC-depleted and xTACC3-depleted extracts with or without add-back extracts, as indicated. Representative images are shown. Tubulin is shown in red and DNA in blue. (B) Western blot of the extracts shown in A with anti-CHC (upper), anti-xTACC3 (middle) and anti- α -tubulin (lower) antibodies as indicated. (C) Relative tubulin fluorescence intensity of the spindle structures shown in A was quantified. (D) Quantification of the percentages of sperm-induced spindle structures (normal bipolar spindles and abnormal spindles) shown in A. Data are means \pm s.d. (C,D). (E) Depletion of CHC results in reduced localization of xTACC3 at spindle poles. The localization of xTACC3 was tested in CHC-depleted extracts as well as in xTACC3-depleted extracts. Representative images are shown; xTACC3 is shown in green, tubulin in red and DNA in blue. Scale bars: 10 μ m.

Thus, we conclude that phosphorylation of xTACC3 at S620 and S626 but not at S33 is required for binding with CHC, targeting to spindle poles and function in RanGTP-mediated bipolar spindle assembly. Moreover, the consistent finding that S33 phosphorylation is not required for all three aspects of the function of TACC3 in proper spindle assembly implies that the interaction between CHC and phosphorylated xTACC3 correlates with targeting of xTACC3 to spindle poles.

CHC recruits xTACC3 to spindle poles assembled in *Xenopus* egg extract

To determine the possible function of the interaction between CHC and xTACC3, we depleted CHC and xTACC3 in CSF extracts and tested the abilities of the extracts to support spindle

assembly (Fig. 3A,B). We observed that these procedures removed more than 80% of CHC and over 90% of xTACC3 (Fig. 3B), and that both CHC- and TACC3-depleted extracts failed to support proper spindle assembly induced by sperm chromatin. Quantification analysis revealed that the total tubulin fluorescence was reduced by approximately 53% and 64% upon depletion of CHC or xTACC3, respectively, and that both proteins contributed to normal bipolar spindle assembly (Fig. 3C,D). The spindle assembly activity in xTACC3-depleted extract was fully restored by the addition of 15 nM xTACC3. We also tested the localization of xTACC3 and observed that, in mock-depleted extracts, xTACC3 localized along the microtubules and poles of the well-assembled spindles (Fig. 3E). In TACC3-depleted extracts, coupled with the defects in bipolar spindle assembly, the presence of xTACC3 on the spindles was largely reduced or absent. When exogenous xTACC3 was added to TACC3-depleted extract, the spindle localization of TACC3 was fully recovered. CHC depletion resulted in a similar defect in bipolar spindle assembly to that of xTACC3 depletion; moreover, the targeting of xTACC3 to spindle poles and microtubules was greatly reduced upon CHC depletion, suggesting that CHC is necessary for the localization of xTACC3 on spindle poles. Together, these data suggest that both CHC and xTACC3 are required for proper spindle assembly and that CHC recruits xTACC3 to spindle poles *in vitro*.

CHC recruits phosphorylated TACC3 to spindle poles for proper spindle assembly and chromosome alignment *in vivo*

We further tested the role of the interaction between TACC3 and CHC in spindle assembly in human somatic cells *in vivo*. Using immunofluorescence, we observed that hTACC3 and CHC were both colocalized on spindles in mitotic human cells (supplementary material Fig. S4A). Using a co-immunoprecipitation assay, we confirmed that CHC interacted with phosphorylated hTACC3 in both human and *Xenopus* cells (supplementary material Fig. S4B,C). In addition, hTACC3 overexpression resulted in the localization of more CHC to the spindle (supplementary material Fig. S4D). Mutation experiments revealed that the phosphorylation of hTACC3 at S552 and S558 (which correspond to S620 and S626, respectively, in xTACC3) is required for its localization on spindle poles (supplementary material Fig. S4E). Together, these data confirm that CHC and TACC3 interact in human cells as in *Xenopus* cells.

Next, we silenced hTACC3 or CHC expression in human cells by RNAi through expressing short hairpin RNA (shRNA). By quantification of the levels of fluorescence intensity, it was found that this procedure reduced the level of hTACC3 by more than 90% in cells transfected with hTACC3 RNAi (Fig. S5A). A knockdown proof (KDP) construct (Royle et al., 2005) expressing hTACC3 that is refractory to the RNAi was able to recover the hTACC3 expression to normal levels (supplementary material Fig. S5A). Similarly, CHC expression was reduced by more than 80% in cells transfected with CHC RNAi; the corresponding KDP construct also recovered the expression level of CHC (supplementary material Fig. S5B). Using this approach, we found that the localization of CHC was not affected by hTACC3 knockdown (Fig. 4A). However, the localization of hTACC3 to the spindle was clearly reduced after CHC knockdown, but was fully restored in cells transfected with CHC KDP (Fig. 4B), consistent with the aforementioned result that CHC targets xTACC3 to spindle poles *in vitro* (Fig. 3E).

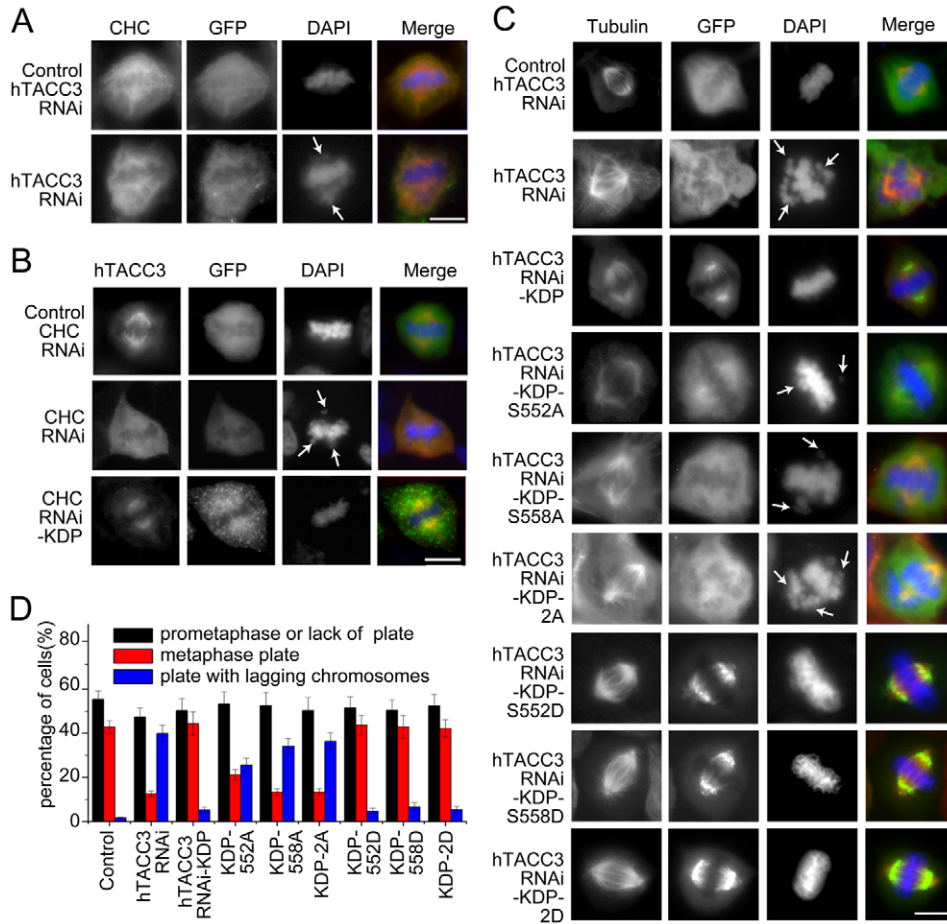


Fig. 4. Recruitment of hTACC3 to spindle poles by clathrin is required for spindle assembly and proper chromosome alignment in human cells. (A) Localization of CHC is not affected upon ablation of hTACC3 by RNAi. 293T cells were fixed and stained 72 hours after transfection. The GFP signals indicated cells with short hairpin RNA (shRNA). (B) hTACC3 fails to localize efficiently at spindle poles in cells in which CHC has been ablated by RNAi, whereas it localizes normally in cells expressing control shRNA and GFP-CHC-KDP (for rescue). (C) Ablation of hTACC3 results in failure of chromosome alignment and minor spindle-assembly defects. WT and phospho-mimetic mutants could rescue the defects, but mutation of either S552 or S558 to alanine failed to reverse the defects caused. Representative images are shown. (D) Percentages of cells shown in C in prometaphase or with lack of metaphase plate, with metaphase plate, and with metaphase plate and lagging chromosomes. Data are means \pm s.d. Scale bars: 10 μ m. Arrows indicate the lagging chromosomes.

We also observed that knockdown of hTACC3 or CHC by RNAi resulted defects in spindle morphology and chromosome alignment (Fig. 4A,B). The defects caused by hTACC3 silencing by RNAi could be rescued by expression of exogenous wild-type hTACC3 and the phospho-mimic hTACC3 mutants S552D, S558D or 2D, but not the non-phosphorylatable mutants S552A, S558A or 2A (Fig. 4C,D). Furthermore, ablation of CHC by RNAi led to defects in spindle assembly and chromosome alignment similar to those found by knockdown of TACC3 (supplementary material Fig. S6). Together, these data indicate that hTACC3 is recruited to spindle poles by CHC for proper spindle assembly and chromosome alignment, and that the phosphorylation of hTACC3 at S552 and S558 is crucial for spindle pole location and function.

In summary, we report that CHC recruits TACC3 to spindle poles for proper spindle assembly and chromosome alignment. We show that, in mitosis, CHC interacts with TACC3 that has been phosphorylated by Aurora A. The interaction between CHC and TACC3 is inhibited by importin β , and this inhibition is overcome by RanGTP. Given the conserved roles, from *Xenopus* to humans, of both TACC3 and CHC during mitosis, we believe that the mechanism by which CHC recruits phosphorylated TACC3 to spindle poles for proper spindle assembly and chromosome alignment is likely to be conserved in other eukaryotes. Nevertheless, how CHC targets phosphorylated TACC3 to spindle poles remains unclear. It also remains to be determined how the spindle-pole-localized TACC3 affects chromosome alignment.

Materials and Methods

cDNA, protein purification and antibodies

pGEX-xTACC3 (maskin) and xTACC3-TACC domain fusion protein (xTACC3-TD; aa 714–931) were provided by Christiane Wiese (O'Brien et al., 2005). pEGFP-hTACC3 was a gift from Chi-Ying F. Huang (Tien et al., 2004). pEGFP-CHC was kindly provided by Stephen J. Royle (Royle and Lagnado, 2006). TACC3 nonphosphorylatable mutants and phospho-mimetic mutants were generated by point mutation. Proteins were purified with glutathione Sepharose 4B (GE Healthcare) or Co²⁺ affinity resin (Clontech) according to the manufacturer's instructions. Rabbit and mouse anti-xTACC3 were generated against purified GST-xTACC3-TD fusion protein. Rabbit anti-importin- β was generated against His-importin β . Rabbit and mouse anti-CHC polyclonal antibodies were generated against purified His-CHC (aa 1–330). Rabbit anti-GFP was generated against His-GFP. The polyclonal antibodies were affinity purified. Other antibodies were as follows: mouse anti- γ -tubulin (Sigma), mouse anti- α -tubulin (Sigma) and mouse anti-hTACC3 (Santa Cruz Biotechnology).

Cell culture, synchronization and transfection

XTC cells were cultured at 23°C in XTC culture medium [70% DMEM (Gibco), 10% fetal bovine serum (FBS) and 2 mM HEPES]. HeLa cells and 293T cells were cultured at 37°C under 5% CO₂ in DMEM supplemented with 10% FBS. To arrest 293T cells in mitosis, thymidine was used to synchronize the cells in early S phase, and they were then released into nocodazole (50 nM) for 14 hours. Approximately 80% of cells were arrested in mitosis on the basis of morphology. Transient cDNA transfections were carried out on cells using Lipofectamine 2000 (Invitrogen) according to the manufacturer's instructions.

CSF extract preparation

Xenopus CSF extracts were prepared as described previously, with little modification (Hannak and Heald, 2006). In brief, the eggs were washed sequentially with XB (10 mM HEPES, 0.1 mM CaCl₂, 100 mM KCl, 1 mM MgCl₂ and 50 mM sucrose, pH 7.8) and CSF-XB buffer (10 mM HEPES, 2 mM MgCl₂, 0.1 mM CaCl₂, 100 mM KCl, 5 mM EGTA and 50 mM sucrose, pH 7.8); next, the eggs were centrifuged in CSF-XB plus cytochalasin B (100 μ g/ml) at 13,000 rpm for 10 minutes (TLS55 rotor, Beckman) to obtain the supernatant.

In vitro spindle and aster assembly, and immunodepletion

Rhodamin-labeled tubulin prepared from pig brain was added to a final concentration of 0.05–0.2 mg/ml. Demembrated *Xenopus* sperm (600 nuclei/ μ l) and RanQ69L (20 μ M) were added to assemble asters and spindles. The samples were fixed and mounted with fixation buffer [Marc's modified ringers (MMR) plus 4% paraformaldehyde and 50% glycerol]. For immunodepletion of xTACC3 and CHC in CSF extracts, 100 μ l Dynal protein A beads coupled with 30 μ g anti-xTACC3 and 50 μ g anti-CHC antibodies were used to deplete 100 μ l extract.

Immunofluorescence and microscopy quantifications

For immunofluorescence of spindles assembled in CSF extract, 10 μ l extract were diluted in 1 ml BRB80 (80 mM PIPES, 1 mM $MgCl_2$, 1 mM EGTA, pH 6.8) containing 25% glycerol and then spun down through 3 ml BRB80/35% glycerol onto coverslips (R10S rotor, 8000 rpm, 10 minutes). Fixation was followed by incubation in methanol at $-20^\circ C$ for 5 minutes before immunofluorescence. Before the immunofluorescence, cells were fixed in PBS/4PFA for 15 minutes and then permeabilized with 0.2% Triton X-100 for 4 minutes, or, alternatively, fixed in cold methanol. Coverslips were blocked in TBS/3% BSA for 10 minutes, incubated with primary antibodies for 1 hour, washed with TBS, incubated with secondary antibodies for 1 hour and washed with TBS. Finally, the DNA was stained with 1 μ g/ml DAPI and slides were analyzed under a Zeiss Axiovert 200M microscope. Images were captured with a Zeiss MRM CCD camera and AxioVision image-acquisition software. The fluorescence intensity was measured by ImageJ software (NCBI). Statistical quantifications were performed using Origin software.

GST co-precipitations

150 μ l CSF extracts were pre-cleared by centrifuge at 6000 rpm (12154-H rotor; Sigma) for 15 minutes. The pre-cleared extract was then incubated with 50 μ g GST or GST-xTACC3 fragments for 30 minutes with rotation. After the addition of 50 μ l glutathione-Sepharose beads, the extracts were incubated for an additional 90 minutes. The beads were collected and washed several times with CSF-XB, and then were analyzed by SDS-PAGE and western blotting.

Co-immunoprecipitation

20 μ l of Protein-A Sepharose beads (GE Healthcare) were washed three times with PBS, and incubated with antibodies for 1 hour at $4^\circ C$ on a rotator. For co-immunoprecipitation from 293T cells, 20 μ g rabbit anti-CHC antibody or 20 μ g rabbit anti-GFP were used. Beads were then washed three times with lysis buffer (0.5% NP-40, 20 mM Tris-HCl, 500 mM NaCl, 0.5 mM EGTA, 10 mM NaF, 2 mM $NaVO_3$, 10 mM β -glycerophosphate, 10 μ g/ml leupeptin, 0.7 μ g/ml pepstatin A, 1.5 μ g/ml aprotinin and 1 mM PMSF, pH 7.4). Cells were lysed on ice for 30 minutes in lysis buffer and followed with centrifugation at 16,000 g for 15 minutes to get the supernatants. The beads were then incubated with the supernatants for 2 hours at $4^\circ C$ on the rotator. After washing with lysis buffer, immunoprecipitates were analyzed. For immunoprecipitation from CSF extracts, 20 μ g rabbit anti-xTACC3 antibody or 20 μ g rabbit anti-CHC were used. The procedures were as described for 293T cells, except that the immunoprecipitation buffer was CSF-XB. Aurora A was added to the cell lysate or CSF extracts as indicated.

Western blotting

Proteins resolved by SDS-PAGE were transferred to nitrocellulose membranes by using Mini Trans-Blot (Bio-Rad). The membranes were blocked in TTBS (TBS plus 0.3% Tween-20) containing 3% milk for 1 hour at $37^\circ C$. Next, they were incubated with a primary antibody in TTBS/milk for 1 hour at $37^\circ C$, washed with TTBS 3 times, blocked with milk for 1 hour at $37^\circ C$, incubated with HRP-conjugated secondary antibody for 1 hour and washed with TTBS 6 times. Blots were developed by chemiluminescence.

RNAi

CHC-RNAi-KDP was a kind gift from Stephen J. Royle, and the pBrain vectors to co-express proteins and shRNA were described previously (Royle et al., 2005). CHC RNAi were subcloned from CHC-RNAi-KDP, which is the same as pBrain-CHC4 as described previously (Royle et al., 2005). The DNA sequence for RNAi was synthesized and ligated into pBrain vectors. The target sequences of TACC3 RNAi were previously reported (Schneider et al., 2007). For TACC3 RNAi rescue constructs (KDP), we used the primers to generate point mutation to the target sequence. Assays for RNAi were performed 72 hours after transfection. The primers are described below.

Control CHC RNAi primers: 5'-GATCCCCGACATTGAAATGAAA-ATTAATCAAGAGATTACTTTTCATTCAATGTCTTTTC-3'; 5'-TCGAGAAAAGACATTGAAATGAAAAGTAATCTTGAATTAATTTTCATTTCAT-ATGTCGGG-3'. Control TACC3 RNAi primers: 5'-GATCCCCGGGAGCAGTTTGA-CTTTCATTTCATGAGAGAGGAAGTCCAACTGCTCCCTTTTC-3'; 5'-TCGAGAAAAGGGAGCAGTTTGAAGTCTTCTGTAATGAAGTCCAACTGCTCCCGGG-3'. TACC3 RNAi primers: 5'-GATCCCCGTGGATTACCTG-GAGCAGTTTCAAGAGAACTGCTCCAGGTAATCCACTTTTTC-3'; 5'-AGCT-TAAAAGTGGATTACCTGGAGCAGTTCTTGAAGTCTCCAGGTAATC-CACGGG-3'. TACC3 RNAi KDP primer to generate point mutation: 5'-AGGTG-

GATTATTTAGAACAGTTTGAAGTCTCC-3'; 5'-GTTCCAACTGTTCTAA-ATAATCCACCTCCGC-3'.

We sincerely thank Christiane Wiese for providing xTACC3 and xTACC3-TD cDNAs and for reviewing the manuscript, Chi-Ying F. Huang for providing hTACC3, and Stephen J. Royle for providing CHC and shRNA vectors. We also thank all the other members of our laboratories for useful comments. This work was supported by funds provided to C.Z. from the National Natural Science Foundation of China (NSFC) (30671063, 30721064, 30900726, 31071188, 31030044 and 90913021) and the State Key Basic Research and Development Plan (2006CB910101, 2007CB914502 and 2010CB833705). P.R.C. is supported by the Biotechnology and Biological Sciences Research Council (BBSRC).

Supplementary material available online at

<http://jcs.biologists.org/cgi/content/full/123/21/3645/DC1>

References

- Albee, A. J., Tao, W. and Wiese, C. (2006). Phosphorylation of maskin by Aurora-A is regulated by RanGTP and importin beta. *J. Biol. Chem.* **281**, 38293–38301.
- Carazo-Salas, R. E., Guarguaglini, G., Gruss, O. J., Segref, A., Karsenti, E. and Mattaj, J. W. (1999). Generation of GTP-bound Ran by RCC1 is required for chromatin-induced mitotic spindle formation. *Nature* **400**, 178–181.
- Dasso, M., Seki, T., Azuma, Y., Ohba, T. and Nishimoto, T. (1994). A mutant form of the Ran/TC4 protein disrupts nuclear function in *Xenopus laevis* egg extracts by inhibiting the RCC1 protein, a regulator of chromosome condensation. *EMBO J.* **13**, 5732–5744.
- Fotin, A., Cheng, Y., Grigorieff, N., Walz, T., Harrison, S. C. and Kirchhausen, T. (2004a). Structure of an auxilin-bound clathrin coat and its implications for the mechanism of uncoating. *Nature* **432**, 649–653.
- Fotin, A., Cheng, Y., Sliz, P., Grigorieff, N., Harrison, S. C., Kirchhausen, T. and Walz, T. (2004b). Molecular model for a complete clathrin lattice from electron cryomicroscopy. *Nature* **432**, 573–579.
- Gergely, F., Karlsson, C., Still, I., Cowell, J., Kilmartin, J. and Raff, J. W. (2000a). The TACC domain identifies a family of centrosomal proteins that can interact with microtubules. *Proc. Natl. Acad. Sci. USA* **97**, 14352–14357.
- Gergely, F., Kidd, D., Jeffers, K., Wakefield, J. G. and Raff, J. W. (2000b). D-TACC: a novel centrosomal protein required for normal spindle function in the early *Drosophila* embryo. *EMBO J.* **19**, 241–252.
- Hannak, E. and Heald, R. (2006). Investigating mitotic spindle assembly and function in vitro using *Xenopus laevis* egg extracts. *Nat. Protoc.* **1**, 2305–2314.
- Jung, C. K., Jung, J. H., Park, G. S., Lee, A., Kang, C. S. and Lee, K. Y. (2006). Expression of transforming acidic coiled-coil containing protein 3 is a novel independent prognostic marker in non-small cell lung cancer. *Pathol. Int.* **56**, 503–509.
- Kaksonen, M., Toret, C. P. and Drubin, D. G. (2005). A modular design for the clathrin- and actin-mediated endocytosis machinery. *Cell* **123**, 305–320.
- Kinoshita, K., Noetzel, T. L., Pelletier, L., Mechtler, K., Drechsel, D. N., Schwager, A., Lee, M., Raff, J. W. and Hyman, A. A. (2005). Aurora A phosphorylation of TACC3/maskin is required for centrosome-dependent microtubule assembly in mitosis. *J. Cell Biol.* **170**, 1047–1055.
- Klebe, C., Bischoff, F. R., Ponstingl, H. and Wittinghofer, A. (1995). Interaction of the nuclear GTP-binding protein Ran with its regulatory proteins RCC1 and RanGAP1. *Biochemistry* **34**, 639–647.
- Lauffart, B., Vaughan, M. M., Eddy, R., Chervinsky, D., DiCioccio, R. A., Black, J. D. and Still, I. H. (2005). Aberrations of TACC1 and TACC3 are associated with ovarian cancer. *BMC Womens Health* **5**, 8.
- LeRoy, P. J., Hunter, J. J., Hoar, K. M., Burke, K. E., Shinde, V., Ruan, J., Bowman, D., Galvin, K. and Ecsedy, J. A. (2007). Localization of human TACC3 to mitotic spindles is mediated by phosphorylation on Ser558 by Aurora A: a novel pharmacodynamic method for measuring Aurora A activity. *Cancer Res.* **67**, 5362–5370.
- O'Brien, L. L., Albee, A. J., Liu, L., Tao, W., Dobrzyn, P., Lizarraga, S. B. and Wiese, C. (2005). The *Xenopus* TACC homologue, maskin, functions in mitotic spindle assembly. *Mol. Biol. Cell* **16**, 2836–2847.
- Peset, I., Seiler, J., Sardon, T., Bejarano, L. A., Rybina, S. and Vernos, I. (2005). Function and regulation of Maskin, a TACC family protein, in microtubule growth during mitosis. *J. Cell Biol.* **170**, 1057–1066.
- Pucadyil, T. J. and Schmid, S. L. (2009). Conserved functions of membrane active GTPases in coated vesicle formation. *Science* **325**, 1217–1220.
- Raff, J. W. (2002). Centrosomes and cancer: lessons from a TACC. *Trends Cell. Biol.* **12**, 222–225.
- Royle, S. J. and Lagnado, L. (2006). Trimerisation is important for the function of clathrin at the mitotic spindle. *J. Cell Sci.* **119**, 4071–4078.
- Royle, S. J., Bright, N. A. and Lagnado, L. (2005). Clathrin is required for the function of the mitotic spindle. *Nature* **434**, 1152–1157.
- Schneider, L., Essmann, F., Kletke, A., Rio, P., Hanenberg, H., Wetzel, W., Schulze-Osthoff, K., Nurnberg, B. and Piekorz, R. P. (2007). The transforming acidic coiled coil 3 protein is essential for spindle-dependent chromosome alignment and mitotic survival. *J. Biol. Chem.* **282**, 29273–29283.

- Stebbins-Boaz, B., Cao, Q., de Moor, C. H., Mendez, R. and Richter, J. D.** (1999). Maskin is a CPEB-associated factor that transiently interacts with eIF-4E. *Mol. Cell* **4**, 1017-1027.
- Tahara, H., Yokota, E., Igarashi, H., Orii, H., Yao, M., Sonobe, S., Hashimoto, T., Hussey, P. J. and Shimmen, T.** (2007). Clathrin is involved in organization of mitotic spindle and phragmoplast as well as in endocytosis in tobacco cell cultures. *Protoplasma* **230**, 1-11.
- Takei, K. and Haucke, V.** (2001). Clathrin-mediated endocytosis: membrane factors pull the trigger. *Trends Cell. Biol.* **11**, 385-391.
- Tien, A. C., Lin, M. H., Su, L. J., Hong, Y. R., Cheng, T. S., Lee, Y. C., Lin, W. J., Still, I. H. and Huang, C. Y.** (2004). Identification of the substrates and interaction proteins of aurora kinases from a protein-protein interaction model. *Mol. Cell. Proteomics* **3**, 93-104.
- Wilde, A. and Zheng, Y.** (1999). Stimulation of microtubule aster formation and spindle assembly by the small GTPase Ran. *Science* **284**, 1359-1362.
- Yamauchi, T., Ishidao, T., Nomura, T., Shinagawa, T., Tanaka, Y., Yonemura, S. and Ishii, S.** (2008). A B-Myb complex containing clathrin and filamin is required for mitotic spindle function. *EMBO J.* **27**, 1852-1862.